Charge-Transfer Kinetics of Alloying in Mg-Sb and Li-Bi Liquid Metal Electrodes

Jocelyn M. Newhouse[*] and Donald R. Sadoway[*,z]

Department of Materials Science and Engineering, Massachusetts Institute of Technology, Cambridge, Massachusetts 02139-4307, USA

Liquid metal batteries (LMBs) comprising electrodes of two different liquid metal alloys separated by a molten salt electrolyte have been shown to be high rate-capability energy storage devices. In an effort to specify the limits of the LMB performance envelope, i.e., the electrical output of the cell, the charge transfer kinetics at the positive electrodes in Li-Bi and Mg-Sb have been characterized by electroanalytical methods. The variation in exchange current density, j_0, with depth of discharge yielded average values of 60 A/cm^2 in Li-Bi and 12 A/cm^2 for Mg-Sb. These values confirm the highly facile nature of the liquid-liquid metal-salt interface and indicate that the current in these cells is not limited by electron transfer.

Recent advancements in liquid metal batteries (LMBs) have demonstrated the feasibility of constructing high rate-capability energy storage devices out of a plurality of liquid alloy combinations of alkali or alkaline-earth metals and metalloids as depicted in Figure 1.[1] As a step toward specifying the limits of the LMB performance envelope, herein we investigate one of the relevant kinetic processes that govern the electrical output of the cell—the charge-transfer reaction at the positive electrode.

As the name suggests, the active components of LMB cells are two liquid metal electrodes separated by a molten salt electrolyte. The three mutually immiscible liquids phase-separate into a vertically layered stack, as shown in Figure 1. Electrochemical processes at liquid metal/molten salt interfaces are by their very nature exceedingly fast. The high temperatures translate to high thermal energies[a] and the liquid-liquid interfaces contribute low activation energies.[2] These two features combine to elevate the standard rate constant of charge transfer, k_0, and thus the exchange current density, j_0, which is a measure of how facile the reaction is. For example, the exchange current densities of two widely studied liquid metal electrodepositions - aluminum at 960°C and magnesium at 750°C - have been measured as 8 and 4 A/cm^2, respectively, for which the general charge transfer reaction can be expressed as

$$M^{z+} + ze^- \rightarrow M(\ell). \qquad [1]$$
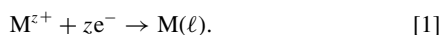
These values would suggest that even at the high charge/discharge rates of LMBs (0.1–1 A/cm^2), charge transfer is sufficiently fast to detract negligibly from the battery performance. However, LMB cell operation is fundamentally different from pure metal deposition, calling into question the ability to make inferences from these data. LMBs not only operate at lower temperatures (400–600°C), but the itinerant species A is deposited into a solvating metal (denoted B, the positive electrode) at much lower activities (10^{-5} - 10^{-7} vs. the pure state), and the charge transfer reaction is now written as

$$A^{z+} + ze^- \rightarrow A(B). \qquad [2]$$
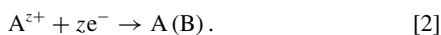
These differences would result in a substantially lower exchange current density for electrochemical alloying/de-alloying than that for pure metal deposition as evident in the defining equation:

$$j_0 = k_0 \frac{a_R^\alpha a_O^{(1-\alpha)}}{\gamma_\ddagger}, \qquad [3]$$

where a_i is the activity of species i and $\gamma_\ddagger$ is the activity coefficient of the activated process.[3]

Electrochemical alloying/de-alloying at liquid electrodes has seen limited study at high temperatures. Castrillejo et al. have explored electrochemical alloying of rare-earth metals at liquid electrodes,[4,5] which exhibit low solubility limits and relatively slow charge transfer kinetics ($k_0 \sim 10^{-3}$ cm/s). Kisza et al. investigated the reaction of sodium at a lead electrode utilizing a combination of chronopotentiometric relaxation and modified electrochemical impedance spectroscopy[6] and reported an exchange current density exceeding 100 A/cm^2 ($k_0 > 0.1$ cm/s). Due to the huge disparity in these k_o values, both measured under alloying conditions, it was deemed prudent to explore electrochemical alloying at liquid alloy electrodes of interest to LMB cells.

Various liquid metal battery chemistries have been tested to date, including Na-Bi,[7] Mg-Sb,[8] Ca(Mg)-Bi,[9] Ca-Sb,[10] Li-Pb-Sb,[11] and Li-Bi.[12] For the purpose of this study, the Mg-Sb and Li-Bi couples were chosen for two main reasons: (1) relative stability with their respective molten salt electrolytes and (2) itinerant ions of different valence: Li$^+$ vs. Mg^{2+}. The charge transfer kinetics of each couple were studied as a function of alloy concentration by the galvanostatic pulse method[13] in a three-electrode cell with a stable two-phase reference electrode.

Experimental

Electrochemical cell.—A schematic of the electrochemical cell used for the galvanostatic pulse measurements is shown in Figure
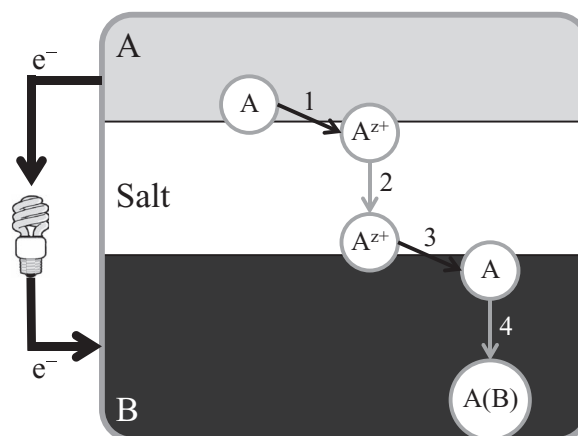

Figure 1. Schematic of a liquid metal battery cell. The negative electrode is comprised of a low density, electropositive metal A and, if desired, other metals A' used to lower the melting temperature. At the positive electrode is a high density, electronegative metal (or alloy) B.

*Electrochemical Society Member.
zE-mail: dsadoway@mit.edu
aThe thermal energy is RT/zF = 26/z mV at 25°C and RT/zF = 75/z mV at 600°C.
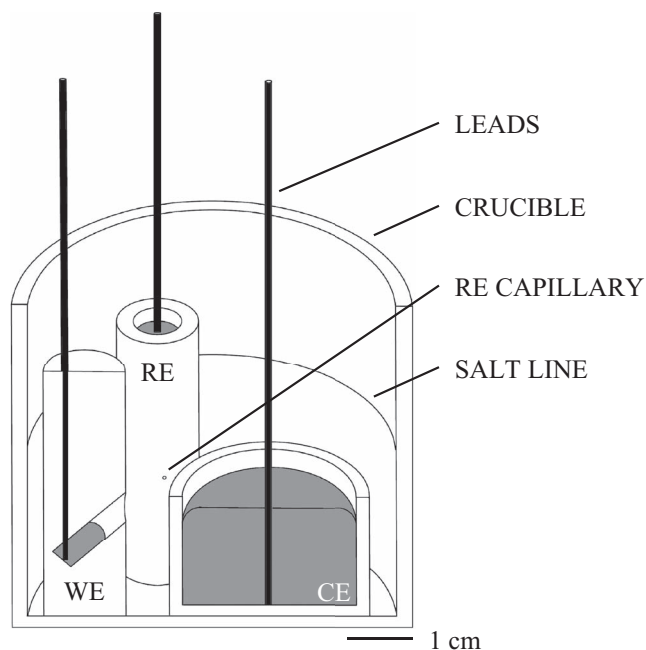
Figure 2. Schematic of three-electrode electrochemical cell. Current flows between the working (WE) and counter (CE) electrodes while the potential at the WE is measured with respect to the reference electrode (RE). Not pictured: second RE, tungsten wire inert electrode, and ASTM type-K thermocouple.

2. Current flows between the working (WE) and counter (CE) electrodes while the potential at the WE is measured with respect to the reference electrode (RE). Two reference electrodes of the same composition were deployed in order to verify stability and accuracy. For the present work, a new WE was designed with a side capillary, eliminating contact between the electrode lead and the electrolyte. In addition to the alloying WE, a tungsten wire served as an inert electrode. The CE provides a source of the itinerant species (Mg or Li) to maintain the electrolyte composition during coulometric titration (see Electrochemical measurements section). The molten salt electrolyte is chosen for its ability to solvate the itinerant ion and for liquidity over the desired temperature range. The temperature was measured with a Chromel-Alumel (ASTM type-K) thermocouple (radial variation < 2°C). The materials used in the construction of electrochemical cells for the Mg-Sb and Li-Bi measurements are presented in Table I.

Materials preparation.—Alloy samples were prepared in a controlled atmosphere glove box (< 0.1 ppm O_2) by induction melting Mg (99.95%, Alfa Aesar) and Sb (99.999%, Alfa Aesar) or Li (99.9%, Aldrich) and Bi (99.999%, Aldrich) in the boron nitride electrode containment (Saint Gobain, binder free). Once the alloys were fully liquid, a tungsten wire (1 mm Ø, 99.95%, Alfa Aesar) was inserted and the alloys were allowed to cool, ensuring intimate contact between the electrode material and the tungsten electrical lead.

The molten salt electrolyte was prepared in the glove box by combining KCl (99.998%, Ultra Dry, Alfa Aesar), NaCl (99.99%, Ultra

Dry, Alfa Aesar), and $MgCl_2$ (99.99%, Ultra Dry, Sigma Aldrich) or LiBr (99.99%, Ultra Dry, Alfa Aesar) and KBr (99.99%, Ultra Dry, Alfa Aesar) in a crucible. The crucible was then placed in the test vessel and dried under vacuum (∼1 Pa) at 80°C (8 h) and 240°C (6 h) in a tube furnace. The vessel was then purged with argon (99.999%, Airgas) before the temperature was increased (740°C for the Mg-Sb system salt and 600°C for the Li-Bi system salt) and held for 3 h under flowing Ar. Once cooled, the salt was removed from the vessel in the glove box and stored until use. All temperature changes were made with a ± 5°C/min ramp rate.

Test vessel.—Electrochemical measurements were carried out in a stainless steel vessel (pictured in Ref. 14) sealed against the external atmosphere. Seven ports were sealed with o-ring compression fittings, and stainless steel baffle plates provided thermal insulation. The induction-melted electrodes were placed in an alumina crucible with the pre-melted salt. Alumina tubes sealed with epoxy electrically insulated the inert tungsten electrode leads from the test vessel. Assembly was performed in the glove box.

Electrochemical measurements.—The drying procedure used for the salt (Materials preparation section) was again performed before bringing the cell to temperature. The two REs equilibrated in less than 2 h, indicating cell stability.

Cyclic voltammetry.—Potential sweeps were performed on the inert (tungsten) electrode to confirm the electrochemical window of the molten salt electrolyte over the potential range of alloying for the Li-Bi and Mg-Sb systems. In addition, potential sweeps at the alloying electrodes were conducted to determine an appropriate cleaning potential.

Coulometric titration.—Coulometric titration was used to change the alloy concentration of the WEs. First the electrode was cleaned at a potential high enough to remove the alloying species without oxidizing the solvent liquid metal. A cathodic current ($I = -14$ mA) was then passed to deposit the desired amount of lithium or magnesium. A rest period of 5,000 s followed to allow for homogenization of the electrode, indicated by a stable open circuit potential (OCP).

The resulting concentration of the liquid alloying electrode, x_A, is given by

$$x_A = \frac{n_A}{n_A + n_B} = \frac{-It/zF}{-It/zF + n_B}, \qquad [4]$$

where n_i is the number of moles of species i in the electrode, I the current, and t the current duration. 100% coulombic efficiency is assumed.

Galvanostatic transients.—To determine the exchange current density of alloying/de-alloying at liquid alloy electrodes of various compositions, galvanostatic pulse measurements were performed after coulometric titration.[13] For the charge transfer reaction

$$O + ze^- \leftrightarrow R,$$
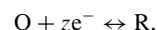
where in this work the oxidized species O is A^{z+} and the reduced species R is A(B), the overpotential transient η after application of a current pulse j_p is

$$\eta = \frac{RT}{zF} j_p \left[\frac{1}{j_0} + \frac{2}{\pi^{1/2}} N t^{1/2} \right], \qquad [5]$$

with

$$N = \frac{1}{zF} \left(\frac{1}{c_O^* D_O^{1/2}} + \frac{1}{c_R^* D_R^{1/2}} \right),$$

where D_i is the diffusion coefficient of species i, and c_i^* the bulk concentration of species i. When using the bulk concentrations, j_0 is the apparent exchange current density. To be precise, the exchange current density is defined in terms of the instant concentration of

Table I. Experimental design for Mg-Sb and Li-Bi electrochemical measurements. All compositions are in mole fraction.

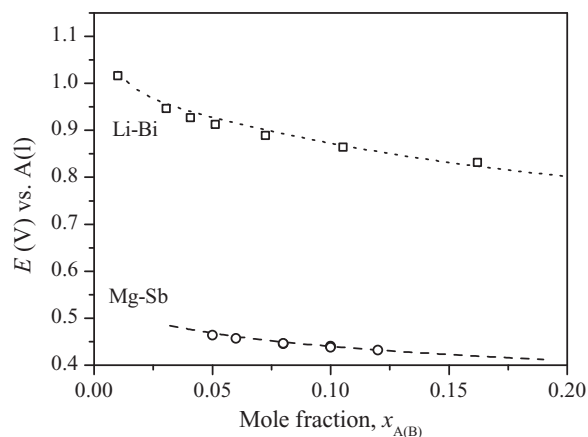|	Mg-Sb	Li-Bi
alloying WE	Sb	Bi
CE	$Mg_{0.15} Sb_{0.85}$	$Li_{0.15} Pb_{0.85}$
RE	$Mg_{0.4} Sb_{0.6}$	$Li_{0.6} Bi_{0.4}$
salt	$(KCl)_{0.4} (NaCl)_{0.2} (MgCl2)_{0.4}$	$(LiBr)_{0.67}(KBr)_{0.33}$
crucible	MgO	$Al_2 O_3$
temperature	660°C	450°C

Figure 3. Potential values from emf studies of Mg-Sb (dash, supplemental information) and Li-Bi (dot,[15]) compared with OCP measurements after coulometric titrations (symbols) for cells described in Table I.

Figure 4. Cyclic voltammograms at tungsten (W) and alloying electrodes for (a) Mg-Sb cell at 660°C (933 K) and (b) Li-Bi cell at 450°C (723 K). Tungsten electrode area of 0.05 cm² assumed. Scan rate 10 mV/s.

Figure 5. Representative overpotential transients for deposition at (a) $Mg_{0.05}Sb_{0.95}$ and (b) $Li_{0.04}Sb_{0.96}$ alloying electrodes. The current density for each pulse is (1) −165; (2) −220; (3) −80; and (4) −140 mA/cm². Lines are linear fits to the curve after the initial non-linearity.

species i at the electrode-electrolyte interface, not in terms of its bulk concentration.[3] The first term in the brackets of Equation 5 is the contribution of the charge-transfer reaction to the overpotential (η_{ct}), and the second term is the time-dependent mass-transport contribution (η_{mt}). This solution to the diffusion equation is valid 50 μs after the current is stopped and assumes semi-infinite one-dimensional diffusion, linear charge-transfer kinetics, negligible non-faradaic current due to double-layer charging, and solubility of O and R in either the electrolyte or the electrode. Care was taken in the experimental design and procedures to ensure that each of the assumptions used in the derivation remained valid (see Ref. 14 for in-depth discussion).

Each galvanostatic pulse had a duration of 0.5 s and consisted of three steps:

(1) OCP step: $I = 0$, (2) transient step: $I = I_p$, and (3) relaxation step: $I = 0$. After a two-minute rest period, the next pulse was initiated. Each sequence consisted of cathodic and anodic current steps of two different magnitudes. Two galvanostatic pulse sequences were performed, separated by a one-hour constant-potential hold. To test if the order of pulses affected the results the set of four pulses was repeated and the order of pulses changed in the second sequence.

Results and Discussion

Thermodynamic behavior.—The OCP after coulometric titrations, E_{cell}, was converted to the potential vs. the standard state (Mg(ℓ) and Li(ℓ) respectively), E_{WE}, via the following relationship

$$E_{WE} = E_{cell} + E_{RE}, \qquad [6]$$

where E_{RE} is determined for the Mg-Sb system from experimental data given in Table S1 and for the Li-Bi system from data reported by Weppner and Huggins.[15]

The resulting values exhibit good agreement to those measured during emf tests (i.e. with chemical, instead of electrochemical, formation of the alloys) (Figure 3). This suggests minimal non-faradaic transport of the itinerant ion.

Cyclic voltammetry.—Cyclic voltammograms at the tungsten and liquid electrodes in both the Mg-Sb and Li-Bi three-electrode cells are shown in Figure 4. Deposition at the alloying electrode occurs at a higher potential than pure metal deposition due to the decrease in activity of the itinerant species A in A-B alloys. In contrast, an inert electrode shows negligible faradaic processes over the same potential range.

Exchange current density measurements.—The exchange current densities of electrochemical alloying/de-alloying at liquid Mg-Sb and Li-Bi electrodes of varying composition were determined using
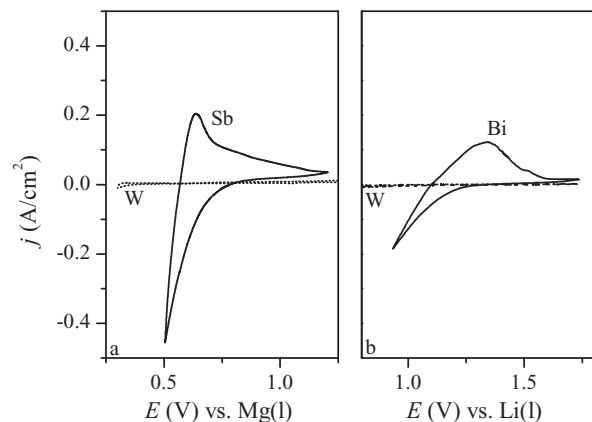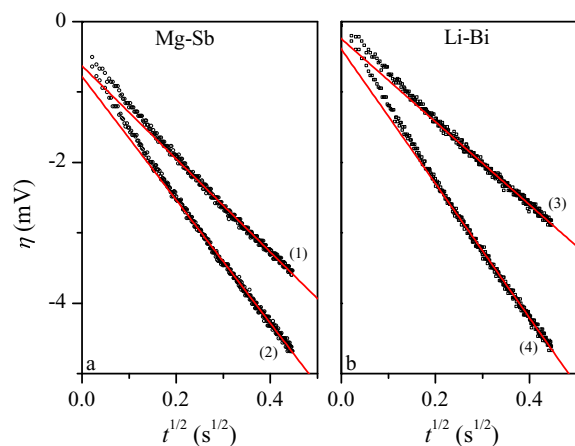
the galvanostatic pulse method described in Galvanostatic transients section. Overpotential transients were corrected for the uncompensated resistance. Linear regression was performed on each η vs $t^{1/2}$ trace and the exchange current density calculated from the intercept ($\eta_{t=0}$) according to Equation 4. Data for which the R² values were greater than 0.97 were included in the analysis.[b] Representative data are presented in Figure 5.

The reproducibility of the transients within sequences was good; however, agreement between sequences was less consistent and thus an average j_0 was calculated for the cathodic and anodic pulses before and after the rest period. Anodic transients exhibited more curvature and less reproducibility than cathodic pulses and are not included in the following discussion. The calculated exchange current densities at alloying electrodes of varying composition are shown in Figure 6.

Error analysis.—The uncertainty in the calculated value of the exchange current density arises from three main sources: (1) reproducibility of the measurements, (2) uncertainty in the measured parameters, and (3) uncertainty in the shape of the electrode surface at high temperature. The following sections discuss the magnitudes of each source of error.

---

[b]For $x_{Mg(Sb)} = 0.12$ this condition was relaxed to R² < 0.95 to enable inclusion of more than one transient.
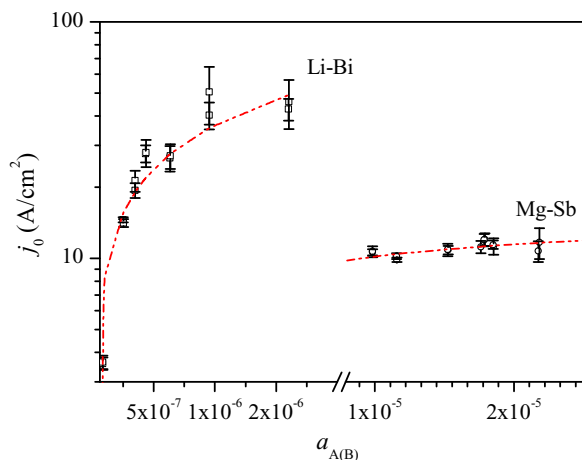
Figure 6. The average exchange current density values for A deposition at A–B liquid alloy electrodes calculated from cathodic current pulses. Lines are fits of the data to $j_0 = C\, a_{A(B)}{}^\alpha$. Error bars indicate the standard deviation for each sequence.

Reproducibility.—The error shown in Figure 6 is the standard deviation of the exchange current density values calculated from the cathodic pulses in a given sequence. The low values of $\eta_{t=0}$ make j_0 values very sensitive to slight changes in the slope of the fitted line (e.g. ± 0.1 mV $\sim 10\%$ of $\eta_{t=0}$). The standard deviation ranges from 2–15% of j_0 for Mg-Sb alloys and 2–27% of j_0 for Li-Bi.

Differential error analysis.—The exchange current density is derived from measured parameters, and the error in those measurements propagates to the calculated value of j_0. Differential error analysis enables calculation of the propagated error. For each transient, the exchange current density is calculated according to

$$j_0 = \frac{RT\,I_p}{zFA\eta_{t=0}}, \qquad [7]$$

where the error in the absolute temperature T ($\Delta T = 2$ K), applied current I_p ($\Delta I_p = 0.05$ mA), electrode surface area A ($\Delta A = 5 \times 10^{-3}$ cm^2), and the intercept of the fit line $\eta_{t=0}$ ($\Delta \eta_{t=0} = 0.091$ mV), each contribute error to the calculation. From differential analysis the error in j_0 due to these measurement uncertainties is about ± 1 A/cm^2.

Systematic error in surface area.—The error in the surface area accounted for in the differential analysis (ΔA) is solely that due to measurement of the capillary diameter. However, the shape of the electrode in the liquid state is unknown and thus the value used for the calculation of current density is an estimate. The error in this estimate is taken to be ± 0.02 cm^2, which would shift the calculated j_0 values up or down by approximately 10% but does not affect the relative positions.

Discussion.—For values of j_0 as large as those found in the present study the question of measurability arises. One way to judge measurability, suggested by Nagy,[16] is to assume that the η_{mt} must be no more than 10 times the η_{ct} for the duration of the current pulse. For a pulse time of 0.2 s this gives a limit on j_0 of $\sim$40 A/cm^2 for Mg-Sb electrodes and $\sim$80 A/cm^2 for Li-Bi electrodes. The j_0 values for Li-Bi level off around 60 A/cm^2, which lends support to this analysis. Thus, although the values are large and exhibit substantial error, some conclusions may be drawn from the above results.

The exchange current density of Li alloying/de-alloying at Li-Bi liquid electrodes exhibits marked dependence on the lithium activity in the alloy. Interfacial kinetic theory predicts a dependence of the exchange current density on the activity of the reduced species of $j_0 \propto a_{A(B)}^\alpha$ (Eq. 3). A fit of the cathodically determined values of j_0 to the power function $j_0 = C a_{A(B)}^\alpha$ is shown in Figure 6, and the parameters are given in Table II. The Li-Bi electrochemical alloying reaction exhibits a transfer coefficient $\alpha > 0.5$, which indicates that the electrostatic state of the activated complex more closely resembles

Table II. Fits of the exchange current density vs. activity to $j_0 = C a_{A(B)}^\alpha$ for Mg-Sb and Li-Bi liquid alloy electrodes.

	C	α	R^2
Mg-Sb	72	0.17	0.53
Li-Bi	1.9×10^5	0.62	0.85

that of the reduced species than that of the oxidized species. Although it is unusual for a charge transfer reaction with a neutral reduced species to have $\alpha > 0.5$,[13] this behavior may be due to the highly ionic character of Li-Bi alloys.[17]

The exchange current density of Mg alloying/de-alloying at Mg-Sb liquid electrodes exhibits a much lower dependence on the magnesium activity in the alloy than is the case for Li at Li-Bi liquid electrodes. A similar fitting of the data gives $\alpha < 0.2$ and a much worse "goodness of fit" as indicated by the adjusted R^2 value. One explanation for the lack of dependence on $a_{Mg(Sb)}$ is that the rate-determining step may not involve the completely reduced Mg species. For deposition of liquid Mg at inert electrodes, Kisza et al.[18] suggest the rate-determining step is the first electron transfer $Mg^{2+} + e^- \rightarrow Mg^+$. If a similar mechanism and rate-determining step are assumed at the Mg-Sb electrode, the invariance of j_0 with $a_{Mg(Sb)}$ is expected.

Conclusions

The measurements made in the present study suggest that the charge-transfer reactions for both Mg at Mg-Sb (660°C) and Li at Li-Bi (450°C) are very rapid so as to have negligible impact on the LMB cell performance.

Acknowledgments

References

1. H. Kim, D. A. Boysen, J. M. Newhouse, B. L. Spatocco, B. Chung, P. J. Burke, D. J. Bradwell, K. Jiang, A. A. Tomaszowska, K. Wang, W. Wei, L. A. Ortiz, S. A. Barriga, S. M. Poizeau, and D. R. Sadoway, "Liquid Metal Batteries: Past, Present, and Future," *Chem. Rev.*, **113** (3), 2075 (2013).
2. H. Gerischer, "Mechanism of electrolytic deposition and dissolution of metals," *Anal. Chem.*, **31**, 3339 (1959).
3. K. J. Vetter, *Electrochemical Kinetics: Theoretical and Experimental Aspects*, New York: Academic Press, 1967.
4. Y. Castrillejo, M. R. Bermejo, P. D. Arocas, F. De la Rosa, and E. Barrado, "Electrode Reaction of Cerium into Liquid Bismuth in the Eutectic LiCl-KCl," *Electrochemistry Tokyo*, **73**, 636 (2005).
5. Y. Castrillejo, M. R. Bermejo, P. D. Arocas, A. M. Martinez, and E. Barrado, "The electrochemical behaviour of the Pr(III)/Pr redox system at Bi and Cd liquid electrodes in molten eutectic LiCl-KCl," *J. Electroanal. Chem.*, **579**, 343 (2005).
6. A. Kisza, "The Kinetics of the Sodium Electrode Reaction in Molten Sodium Chloride," *J. Electrochem. Soc.*, **142**, 1035 (1995).
7. E. J. Cairns, C. E. Crouthamel, A. K. Fischer, M. S. Foster, J. C. Hesson, C. E. Johnson, H. Shimotake, and A. D. Tevebaugh, "Galvanic cells with fused-salt electrolytes," Argonne National Laboratory, Argonne, Illinois, 1967.
8. D. Bradwell, H. Kim, A. H. C. Sirk, and D. R. Sadoway, "Magnesium-antimony liquid metal battery for stationary energy storage," *J. Am. Chem. Soc.*, **134**, 1895 (2012).
9. H. Kim, D. A. Boysen, T. Ouchi, and D. R. Sadoway, "Calcium-bismuth electrodes for large-scale energy storage (liquid metal batteries)," *J. Power Sources*, **241**, 239 (2013).
10. T. Ouchi, H. Kim, X. Ning, and D. R. Sadoway, "Calcium-Antimony Alloys as Electrodes for Liquid Metal Batteries," *J. Electrochem. Soc.*, **161**(12), A1898 (2014).
11. K. Wang, K. Jiang, B. Chung, T. Ouchi, P. J. Burke, D. A. Boysen, D. J. Bradwell, H. Kim, U. Muecke, and D. R. Sadoway, "Lithium-antimony-lead liquid metal battery for grid-level storage," *Nature*, **514**(7522), 348 (2014).
12. X. Ning, S. Phadke, B. Chung, H. Yin, P. Burke, and D. R. Sadoway, "Self-healing Li-Bi liquid metal battery for grid-scale energy storage," *J. Power Sources*, **275**, 370 (2015).
13. A. J. Bard and L. R. Faulkner, *Electrochemical Methods: Fundamentals and Applications*, 2nd ed. John Wiley & Sons, Inc., 2001.
14. J. M. Newhouse, Modeling the Operating Voltage of Liquid Metal Battery Cells, *Massachusetts Institute of Technology*, 2014.
15. W. Weppner and R. A. Huggins, "Thermodynamic Properties of the Intermetallic Systems Lithium-Antimony and Lithium-Bismuth," *J. Electrochem. Soc.*, **125**, 714 (1978).

16. Z. Nagy, "D. C. Relaxation Techniques in Electrode Kinetics," in *Modern Aspects of Electrochemistry*, vol. **21**, R. R. Adzic, R. E. White, J. O. Bockris, and B. E. Conway, Eds. ,Plenum Press, 1990, p. 137.

17. G. Steinleitner, W. Freyland, and F. Hensel, "Electrical conductivity and excess volume of the liquid alloy system Li-Bi," *Ber. Bunsenges. Phys. Chem.*, **79**, 1186 (1975).

18. A. Kisza, J. Kazmierczak, B. Borresen, G. M. Haarberg, and R. Tunold, "Kinetics and Mechanism of the Magnesium Electrode Reaction in Molten $MgCl_2$-NaCl Binary Mixtures," *J. Electrochem. Soc.*, **144**, 1646 (1997).

19. J. Sangster and A. D. Pelton, "The Bi-Li (Bismuth-Lithium) system," *JPE*, **12**, 447 (1991).

20. M. S. Foster, S. E. Wood, and C. E. Crouthamel, "Thermodynamics of Binary Alloys. I. The Lithium-Bismuth System," *Inorg. Chem.*, **3**, 1428 (1964).

21. M. L. Saboungi, J. Marr, and M. Blander, "Thermodynamic properties of a quasi-ionic alloy from electromotive force measurements: The LiPb system," *J. Chem. Phys.*, **68**, 1375 (1978).

22. W. Gasior and Z. Moser, "Thermodynamic study of liquid lithium-lead alloys using the emf method," *J. Nucl. Mater.*, **294**, 7783 (2001).

23. R. Hultgren, P. D. Desai, D. T. Hawkins, M. Gleiser, and K. K. Kelley, *Selected Values of the Thermodynamic Properties of the Elements*, Metals Park, OH: American Society For Metals, 1973.